Journal of Molecular Spectroscopy **215,** 262–268 (2002)
doi:10.1006/jmsp.2002.8643

# High-Resolution Fourier Transform Spectroscopy of Three Near-Infrared Transitions of NiF

B. Pinchemel,* T. Hirao,†,[1] and P. F. Bernath†

*Laboratoire de Physique des Lasers, Atomes et Molécules, UMR CNRS 8523 Centre d'Etudes et de Recherches Laser et Applications, Université de Lille I 59655, Villeneuve d'Ascq Cedex, France; and †Department of Chemistry, University of Waterloo, Waterloo, Ontario, Canada N2L 3G1

Received March 22, 2002; in revised form June 13, 2002

The emission spectrum of the NiF radical has been recorded by high-resolution Fourier transform spectroscopy in the region 6000–12 000 $cm^{-1}$. Numerous new near-infrared bands were observed. In this paper three electronic transitions are analyzed leading to the identification of two new electronic states: a $[12.0]^2\Phi_{7/2}$ state and a $[11.1]^2\Pi_{3/2}$ state located, respectively, at 12 008.89 and 11 096.05 $cm^{-1}$ above the $X^2\Pi_{3/2}$ ground state. These electronic states can be correlated to the $[3d^8(^3F)4s]^2F$ atomic term of $Ni^+$ as predicted by Carette *et al.* [*J. Mol. Spectrosc.* **161,** 323–335 (1993)]. 

## I. INTRODUCTION

Recently several papers were devoted to the study of NiF: Tanimoto *et al.* (*1*) published a study of the microwave spectrum, which provided very accurate parameters for the two lower electronic states ($X^2\Pi_{3/2}$ and $[0.25]^2\Sigma^+$). Molecular beam experiments were also performed, and they led to the identification of new excited electronic states and the observation of the vibrational structure for numerous transitions (*2–4*). A high-resolution survey of the visible spectrum of NiF has also been recorded by Fourier transform spectroscopy (FTS) (*5*), leading to the reanalysis of numerous transitions studied previously (references to the many papers published on NiF before 1997 are listed in Ref. (*5*)).

The presence of five spin–orbit components ($X^2\Pi_{3/2}$, $[0.25]^2\Sigma$, $[0.83]^2\Delta_{5/2}$, $[1.5]^2\Sigma^+$, and $[2.2]^2\Delta_{3/2}$) of three electronic states in the energy range 0–2500 $cm^{-1}$ above the $X^2\Pi_{3/2}$ ground state is now well established. The combination of microwave and optical FTS data in the fits improved the accuracy of the parameters of the electronic states studied in Ref. (*5*). As a consequence, any transition involving one of the five low-lying states can now be studied easily.

A theoretical study performed using the ligand field approach (*6*) showed that the electronic states of NiF are strongly correlated with the atomic structure of the nickel ion. Such a ligand field calculation is not expected to provide an absolute correspondence between the experimental and the theoretical energy level diagrams, but at least qualitative agreement is expected. For example, it is experimentally established that most of the identified excited electronic states are located between 18 000 and 21 000 $cm^{-1}$. The theoretical diagram suggests that numerous electronic states are expected in this energy range, and that they are associated with the $[3d^8(^3P)4s]^4P + [3d^8(^1D)4s]^2D$ atomic states of the nickel ion.

A second group of doublet electronic states is expected in the energy range 5000–9000 $cm^{-1}$, which are associated with the $[3d^8(^3F)4s]^2F$ atomic state of $Ni^+$. It was therefore desirable to record the near-infrared spectral region in order to observe transitions between these states and the five already known lower states of NiF.

Numerous transitions have been observed in the spectral range 6000–12 000 $cm^{-1}$. In this paper, we describe the analysis of three electronic transitions located at 10 852, 11 100, and 11 180 $cm^{-1}$ (Fig. 1). It has been possible to identify the nature of the lower states of these transitions and, as a consequence, to locate two new upper states in the energy level diagram (at 11 096.05 $cm^{-1}$ and 12 008.89 $cm^{-1}$).

## II. EXPERIMENTAL DETAILS

All the experiments were carried out at the University of Waterloo. The spectra of NiF were recorded in emission with a Bruker IFS 120 HR Fourier transform spectrometer (*5*). A $CaF_2$ beamsplitter and a silicon photodiode detector were used for a wide survey between 9500 and 13 000 $cm^{-1}$ at a resolution of 0.03 $cm^{-1}$. A 695-nm red pass filter (CORION) was inserted into the sample chamber to minimize the influence of scattered light from the internal He–Ne laser on the spectra. The molecular emission source was a tube furnace combined with a DC discharge. The central part of an alumina tube was heated to 930°C by the high-temperature furnace. A few grams of $NiF_2$ were placed in the center of the alumina tube. A slow flow of Ar buffer gas (7.5 Torr) was used and a DC glow discharge at a current of 0.3 A inside the tube was observed.

Line positions were determined with the PC program "WSpectra" developed by Dr. M. Carleer of the Université Libre

[1] Present address: Institute for Astrophysics and Planetary Sciences, Ibaraki University, 2-1-1 Bunkyo, Mito, Ibaraki, 310-8512, Japan.



0022-2852/02 $35.00

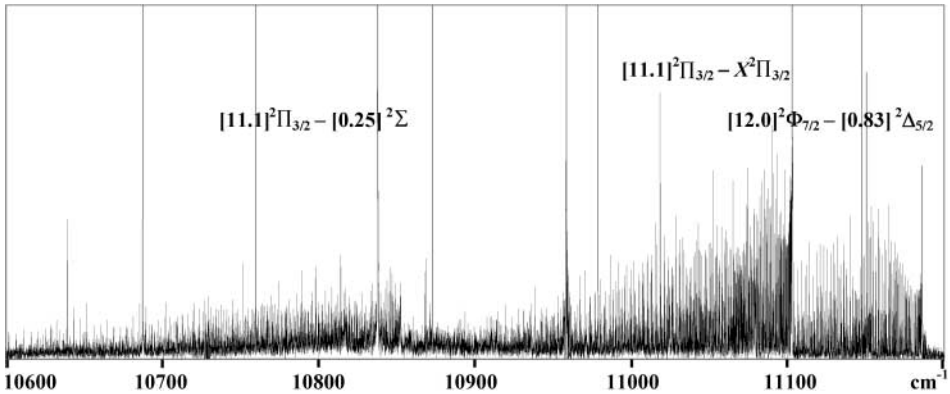


**FIG. 1.** A compressed spectrum of the $\Delta v = 0$ sequences of the three studied transitions.

de Bruxelles, Belgium. Because the spectrometer was not evacuated, air–vacuum corrections were made on all lines (*7*). The spectra were then calibrated by a comparison of the observed Ar atomic lines with standard line positions (*8*). The calibration factor was obtained as 1.000 001 009(68). Observed line positions are listed in Table 1.

## III. DESCRIPTION OF THE BANDS AND ROTATIONAL ANALYSIS

### *(a) The 11 180 cm$^{-1}$ Transition*

This intense band is characterized by well-developed $R$ and $Q$ branches and a weak $P$ branch (Table 1). No fine structure is observed despite the fact that the $R$ branch can be followed up to $J = 75.5$. The derived parameters collected in Table 2 show that the lower state is undoubtedly the $[0.83]^2\Delta_{5/2}$ spin–orbit component. The upper state is therefore at 12 008.92 cm$^{-1}$ above the ground state in the energy level diagram. No transition linking this new state to any of the four other low-lying spin–orbit components can be observed. The intensity of the transition suggests that it is an allowed transition between components of two doublet states. The presence of a strong $Q$ branch indicates that the upper state is either a $^2\Pi_{3/2}$ or a $^2\Phi_{7/2}$ state. A $^2\Pi_{3/2}$ should be linked by intense transitions to one or more of the $X^2\Pi_{3/2}$, the $[0.25]^2\Sigma$, and the $[1.5]B^2\Sigma^+$ states. As already noted, no trace of these transitions was observed. However, a $[12.0]^2\Phi_{7/2}$ state cannot be linked to $X^2\Pi$ or $^2\Sigma$ electronic states. In addition, the intensity of the $R$ branch is expected to be higher than that of the $P$ branch in a $\Delta\Lambda = +1$ transition, as observed (*9*). Such a $^2\Phi_{7/2}$ state is expected to be found in the group of molecular states correlated with the $^2F$ state of the $Ni^+$ ion (*6*). Observation of the $R$ $(J = 2.5)$ line as the first line of the $R$ branch is in agreement with the assignment, although we did not observe the first $P$ line.

It has been possible to observe the 1–1, 0–1, and 1–0 bands for the $[12.0]^2\Phi_{7/2}$–$[0.83]^2\Delta_{5/2}$ transition. The 0–1 band was identified first, although it is blended with another band. This transition has a large value for $\Delta B$ ($|B' - B''| > 0.02$ cm$^{-1}$ and $|B' - B''| < 0.012$ cm$^{-1}$ for all the other studied transitions of NiF) and results in a characteristic pattern with widely spaced lines. The derived rotational parameters are in agreement with the already known values for the $[0.83]^2\Delta_{5/2}$ $(v = 1)$ level (*5*). The $\Delta G_{1/2} = 653.32$ cm$^{-1}$ value agrees with the $\Delta G_{1/2} = 652.68$ cm$^{-1}$ value which has been calculated for the $\Omega = 3/2$ spin–orbit component of the $A^2\Delta$ state (*10*). Combining the new $\Delta G_{1/2}$ value for the $[0.83]^2\Delta_{5/2}$ state with the results published in Ref. (*5*), it is now possible to locate the term values $T_1$ for the $[18.1]^2\Delta_{5/2}$ $(v = 1)$ state: $T_1 = 18\,764.028$ cm$^{-1}$ (18 763.78 cm$^{-1}$ in Ref. (*4*)) and for the $[19.9]\Omega = 5/2$ $(v = 1)$ state: $T_1 = 20\,638.626$ cm$^{-1}$ (20 639.08 cm$^{-1}$ in Ref. (*4*)). We also observed $Q$ and $R$ branches of the 1–1 band but only the $Q$ branch of the very weak 1–0 band. All the experimental data collected (Table 1) for the four bands of the $[12.0]^2\Phi_{7/2}$–$[0.83]^2\Delta_{5/2}$ transition have been fitted simultaneously, and the derived parameters are listed in Table 2. For the upper $[12.0]^2\Phi_{7/2}$ state we obtain $\Delta G_{1/2} = 620.92$ cm$^{-1}$.

### *(b) The 11 100 cm$^{-1}$ Transition*

The 11 100 cm$^{-1}$ transition is even more intense than the nearby 11 180 cm$^{-1}$ transition. We observe two $R$ branches and two $P$ branches (Table 1), and the absence of a $Q$ branch suggests that $\Delta\Omega = 0$. The 331 experimental lines have been fitted and the parameters derived for the lower state are quite similar to those of the $X^2\Pi_{3/2}$ state. A final fit was then carried out including the pure rotational data provided by Tanimoto *et al.* (*1*). Based on the intensity and the observed branches, the new band is an allowed $[11.1]^2\Pi_{3/2}$–$X^2\Pi_{3/2}$ transition. In the fitting procedure, the energy levels of the upper and lower states are represented by simple polynomial expressions. For a $\Omega = 3/2$ spin–orbit component of a $^2\Pi$ state, the $\Lambda$-doubling splitting is expected to be proportional to $J^3$. It turns out that the quality of the fit is greatly improved if the $\Lambda$-doubling part of the energy level formula is described by the expression:

$$E_\Lambda = \pm\frac{a}{2} \pm \frac{p}{2}(J + 0.5) \pm \frac{p_J}{2}J(J + 1)(J + 0.5). \quad [1]$$

In this expression, the upper sign refers to the $e$ levels and the lower sign to the $f$ levels.

Similar phenomenological fitting parameters have already been required for some of the electronic states of NiF (*5*). The explanation for these unusual parameters is the presence of nearby perturbing electronic states. The proof for this suggestion would require a fitting procedure that includes the Hamiltonian matrices of all the interacting states and the coupling matrix elements. We are not at a stage yet for which such a fit is possible. Another sign of possible perturbations is the fact that the $P_{ee}$ and $R_{ee}$ branches can be followed up to $J \approx 92.5$, while the $P_{ff}$ and $R_{ff}$ branches are observed up to only $J \approx 79.5$. Therefore, the lines with $J$ greater than 79.5 show increasing deviations from the expected calculated positions, but the weakness of the lines and the overlapping of this spectral region by the lines of the $Q_{fe}$ and $R_{ee}$ branches of the $[11.1]^2\Pi_{3/2}(v=0)$–$[0.25]^2\Sigma(v=0)$ transition did not allow us to characterize the perturbation (see Fig. 1). We note that this perturbation is not responsible for the presence of the phenomenological $a$ and $p$ parameters, because these parameters are required to account for the line positions even at low $J$ values.

**TABLE 1**
**Observed Line Positions (in $cm^{-1}$) for the Three Studied Transitions of the $^{58}$NiF Isotopomer**

$[12.0]^2\Phi_{7/2}(v'=0)$–$[0.83]A^2\Delta_{5/2}(v''=0)$

| $J$ | $Q$ | $R$ | $P$ | $J$ | $Q$ | $R$ |
|---|---|---|---|---|---|---|
| 2.5 | | 11181.812 | | 40.5 | 11141.509 | 11171.734 |
| 3.5 | 11179.088 | 11182.384 | | 41.5 | 11139.640 | 11170.588 |
| 4.5 | 11178.886 | 11182.913 | | 42.5 | 11137.710 | 11169.378 |
| 5.5 | 11178.625 | 11183.394 | | 43.5 | 11135.750 | 11168.138 |
| 6.5 | 11178.343 | 11183.835 | | 44.5 | 11133.754 | 11166.856 |
| 7.5 | 11178.004 | 11184.230 | | 45.5 | 11131.709 | 11165.523 |
| 8.5 | 11177.620 | 11184.575 | | 46.5 | 11129.612 | 11164.171 |
| 9.5 | 11177.189 | 11184.878 | 11170.242 | 47.5 | 11127.477 | 11162.735 |
| 10.5 | 11176.715 | 11185.132 | 11169.035 | 48.5 | 11125.295 | 11161.270 |
| 11.5 | 11176.196 | 11185.347 | 11167.780 | 49.5 | 11123.069 | 11159.763 |
| 12.5 | 11175.631 | 11185.514 | 11166.491 | 50.5 | 11120.798 | 11158.210 |
| 13.5 | 11175.021 | | 11165.148 | 51.5 | 11118.484 | 11156.600 |
| 14.5 | 11174.365 | | 11163.760 | 52.5 | 11116.124 | 11154.968 |
| 15.5 | 11173.663 | | 11162.331 | 53.5 | 11113.718 | 11153.277 |
| 16.5 | 11172.918 | | 11160.852 | 54.5 | 11111.274 | 11151.541 |
| 17.5 | 11172.126 | 11185.648 | 11159.328 | 55.5 | 11108.782 | 11149.761 |
| 18.5 | 11171.290 | 11185.541 | 11157.748 | 56.5 | 11106.245 | 11147.937 |
| 19.5 | 11170.409 | 11185.397 | 11156.152 | 57.5 | 11103.665 | 11146.071 |
| 20.5 | 11169.483 | 11185.201 | 11154.498 | 58.5 | | 11144.152 |
| 21.5 | 11168.511 | 11184.955 | 11152.796 | 59.5 | | 11142.194 |
| 22.5 | 11167.495 | 11184.670 | 11151.052 | 60.5 | | 11140.191 |
| 23.5 | 11166.433 | 11184.337 | 11149.261 | 61.5 | | 11138.148 |
| 24.5 | 11165.329 | 11183.955 | 11147.415 | 62.5 | | 11136.046 |
| 25.5 | 11164.171 | 11183.533 | 11145.546 | 63.5 | | 11133.908 |
| 26.5 | 11162.978 | 11183.062 | 11143.613 | 64.5 | | 11131.708 |
| 27.5 | 11161.738 | 11182.549 | 11141.656 | 65.5 | | 11129.500 |
| 28.5 | 11160.451 | 11181.987 | 11139.639 | 66.5 | | 11127.226 |
| 29.5 | 11159.118 | 11181.383 | 11137.584 | 67.5 | | 11124.910 |
| 30.5 | 11157.747 | 11180.732 | 11135.480 | 68.5 | | 11122.555 |
| 31.5 | 11156.321 | 11180.037 | 11133.331 | 69.5 | | 11120.166 |
| 32.5 | 11154.857 | 11179.296 | 11131.141 | 70.5 | | 11117.692 |
| 33.5 | 11153.348 | 11178.509 | 11128.904 | 71.5 | | 11115.189 |
| 34.5 | 11151.792 | 11177.684 | 11126.628 | 72.5 | | 11112.646 |
| 35.5 | 11150.194 | 11176.804 | 11124.303 | 73.5 | | 11110.074 |
| 36.5 | 11148.547 | 11175.885 | 11121.936 | 74.5 | | 11107.452 |
| 37.5 | 11146.862 | 11174.925 | 11119.529 | 75.5 | | 11104.787 |
| 38.5 | 11145.115 | 11173.898 | | | | |
| 39.5 | 11143.334 | 11172.837 | | | | |

$[12.0]^2\Phi_{7/2}$–$[0.83]A^2\Delta_{5/2}$

| $J$ | $Q$ | $R$ | $J$ | $R$ | $J$ | $Q$ |
|---|---|---|---|---|---|---|
| | | $v'=1-v''=1$ | | | | $v'=1-v''=0$ |
| 3.5 | | 11149.968 | 44.5 | 11135.530 | | |
| 4.5 | | 11150.510 | 45.5 | 11134.234 | 4.5 | 11799.734 |
| 5.5 | 11146.249 | 11150.982 | 46.5 | 11132.919 | 5.5 | 11799.467 |
| 6.5 | 11145.972 | 11151.425 | 47.5 | 11131.558 | 6.5 | 11799.123 |
| 7.5 | 11145.647 | 11151.831 | 48.5 | 11130.157 | 7.5 | 11798.738 |
| 8.5 | 11145.275 | 11152.174 | 49.5 | 11128.708 | 8.5 | 11798.330 |
| 9.5 | 11144.853 | 11152.483 | 50.5 | 11127.224 | 9.5 | 11797.834 |
| 10.5 | 11144.401 | 11152.751 | 51.5 | 11125.679 | 10.5 | 11797.312 |
| 11.5 | 11143.888 | 11152.973 | 52.5 | 11124.093 | 11.5 | 11796.733 |
| 12.5 | 11143.334 | 11153.137 | 53.5 | 11122.454 | 12.5 | 11796.094 |
| 13.5 | 11142.746 | 11153.277 | 54.5 | 11120.797 | 13.5 | 11795.414 |
| 14.5 | 11142.110 | | 55.5 | 11119.087 | 14.5 | 11794.686 |
| 15.5 | 11141.435 | | 56.5 | 11117.322 | 15.5 | 11793.908 |
| 16.5 | 11140.709 | | 57.5 | 11115.513 | 16.5 | 11793.058 |
| 17.5 | 11139.939 | | 58.5 | 11113.683 | 17.5 | 11792.177 |
| 18.5 | 11139.118 | 11153.277 | 59.5 | 11111.783 | 18.5 | 11791.246 |
| 19.5 | 11138.269 | 11153.137 | | | 19.5 | 11790.266 |
| 20.5 | 11137.365 | 11152.973 | | | 20.5 | 11789.228 |
| 21.5 | 11136.424 | 11152.751 | | | 21.5 | 11788.133 |
| 22.5 | 11135.436 | 11152.483 | | | 22.5 | 11787.000 |
| 23.5 | 11134.407 | 11152.174 | | | 23.5 | 11785.803 |
| 24.5 | 11133.332 | 11151.831 | | | 24.5 | 11784.569 |
| 25.5 | 11132.204 | 11151.425 | | | 25.5 | 11783.279 |
| 26.5 | 11131.046 | 11150.982 | | | 26.5 | 11781.946 |
| 27.5 | 11129.842 | 11150.510 | | | 27.5 | 11780.554 |
| 28.5 | 11128.591 | 11149.968 | | | 28.5 | 11779.116 |
| 29.5 | 11127.300 | 11149.396 | | | 29.5 | 11777.628 |
| 30.5 | 11125.960 | 11148.779 | | | 30.5 | 11776.094 |
| 31.5 | 11124.579 | 11148.114 | | | 31.5 | 11774.499 |
| 32.5 | 11123.152 | 11147.424 | | | 32.5 | 11772.862 |
| 33.5 | 11121.685 | 11146.669 | | | 33.5 | 11771.161 |
| 34.5 | 11120.166 | 11145.872 | | | 34.5 | 11769.435 |
| 35.5 | 11118.614 | 11145.028 | | | 35.5 | 11767.626 |
| 36.5 | 11117.028 | 11144.153 | | | 36.5 | 11765.779 |
| 37.5 | 11115.374 | 11143.228 | | | | |
| 38.5 | 11113.684 | 11142.260 | | | | |
| 39.5 | 11111.946 | 11141.249 | | | | |
| 40.5 | 11110.186 | 11140.191 | | | | |
| 41.5 | 11108.372 | 11139.092 | | | | |
| 42.5 | 11106.514 | 11137.947 | | | | |
| 43.5 | 11104.610 | 11136.754 | | | | |

**TABLE 1**—*Continued*

$[12.0]^2\Phi_{7/2}(v'=0)$–$[0.83]A^2\Delta_{5/2}(v''=1)$

| $J$ | $Q$ | $P$ | $R$ | $J$ | $Q$ | $P$ | $R$ |
|---|---|---|---|---|---|---|---|
| 2.5 | | | 10528.517 | 30.5 | 10507.613 | 10485.356 | 10530.598 |
| 3.5 | | | 10529.113 | 31.5 | 10506.398 | 10483.412 | 10530.117 |
| 4.5 | 10525.644 | | 10529.674 | 32.5 | 10505.150 | 10481.438 | 10529.590 |
| 5.5 | 10525.436 | | 10530.196 | 33.5 | 10503.861 | 10479.410 | 10529.026 |
| 6.5 | 10525.187 | | 10530.675 | 34.5 | 10502.537 | 10477.380 | 10528.423 |
| 7.5 | 10524.899 | | 10531.122 | 35.5 | 10501.169 | 10475.292 | 10527.782 |
| 8.5 | 10524.565 | 10518.345 | 10531.521 | 36.5 | 10499.770 | 10473.154 | 10527.105 |
| 9.5 | 10524.207 | 10517.269 | 10531.884 | 37.5 | 10498.319 | 10470.993 | 10526.386 |
| 10.5 | 10523.799 | 10516.115 | 10532.209 | 38.5 | 10496.846 | 10468.785 | 10525.627 |
| 11.5 | 10523.350 | 10514.927 | 10532.502 | 39.5 | 10495.329 | 10466.549 | 10524.833 |
| 12.5 | 10522.871 | 10513.720 | | 40.5 | 10493.772 | 10464.266 | 10524.001 |
| 13.5 | 10522.362 | 10512.489 | 10532.956 | 41.5 | 10492.178 | 10461.953 | 10523.125 |
| 14.5 | 10521.794 | 10511.180 | | 42.5 | 10490.547 | | 10522.225 |
| 15.5 | 10521.200 | 10509.856 | | 43.5 | 10488.876 | | 10521.266 |
| 16.5 | 10520.557 | 10508.503 | | 44.5 | 10487.170 | | 10520.277 |
| 17.5 | 10519.884 | 10507.081 | | 45.5 | 10485.428 | | 10519.250 |
| 18.5 | 10519.173 | 10505.644 | | 46.5 | 10483.643 | | 10518.182 |
| 19.5 | 10518.413 | 10504.150 | | 47.5 | 10481.822 | | 10517.087 |
| 20.5 | 10517.626 | 10502.645 | 10533.353 | 48.5 | 10479.960 | | 10515.935 |
| 21.5 | 10516.796 | 10501.090 | 10533.248 | 49.5 | 10478.059 | | 10514.764 |
| 22.5 | 10515.935 | 10499.488 | 10533.093 | 50.5 | 10476.137 | | |
| 23.5 | 10515.024 | 10497.858 | 10532.922 | 51.5 | 10474.168 | | |
| 24.5 | 10514.084 | 10496.178 | 10532.721 | 52.5 | 10472.142 | | |
| 25.5 | 10513.102 | 10494.474 | 10532.466 | 53.5 | 10470.104 | | |
| 26.5 | 10512.077 | 10492.724 | 10532.157 | 54.5 | 10468.022 | | |
| 27.5 | 10511.018 | 10490.936 | 10531.829 | 55.5 | 10465.892 | | |
| 28.5 | 10509.924 | 10489.106 | 10531.457 | 56.5 | 10463.749 | | |
| 29.5 | 10508.786 | 10487.240 | 10531.054 | 57.5 | 10461.544 | | |

$[11.1]^2\Pi_{3/2}(v'=0)$–$X^2\Pi_{3/2}(v''=0)$

| $J$ | $P_{ee}$ | $P_{ff}$ | $R_{ee}$ | $R_{ff}$ | $J$ | $P_{ee}$ | $P_{ff}$ | $R_{ee}$ | $R_{ff}$ |
|---|---|---|---|---|---|---|---|---|---|
| 1.5 | | | 11097.841 | 11097.841 | 29.5 | 11056.276 | 11055.587 | 11100.226 | 11099.527 |
| 2.5 | 11094.065 | 11094.065 | 11098.472 | 11098.472 | 30.5 | 11054.334 | 11053.574 | 11099.740 | 11098.967 |
| 3.5 | 11093.188 | 11093.188 | 11099.057 | 11099.057 | 31.5 | 11052.352 | 11051.516 | 11099.216 | 11098.369 |
| 4.5 | 11092.271 | 11092.271 | 11099.606 | 11099.606 | 32.5 | 11050.333 | 11049.420 | 11098.651 | 11097.721 |
| 5.5 | 11091.300 | 11091.300 | 11100.110 | 11100.110 | 33.5 | 11048.278 | 11047.274 | 11098.054 | 11097.034 |
| 6.5 | 11090.299 | 11090.299 | 11100.574 | 11100.574 | 34.5 | 11046.186 | 11045.093 | 11097.417 | 11096.302 |
| 7.5 | 11089.259 | 11089.259 | 11100.999 | 11100.999 | 35.5 | 11044.057 | 11042.862 | 11096.742 | 11095.530 |
| 8.5 | 11088.161 | 11088.161 | 11101.374 | 11101.374 | 36.5 | 11041.891 | 11040.600 | 11096.028 | 11094.711 |
| 9.5 | 11087.049 | 11087.049 | 11101.724 | 11101.724 | 37.5 | 11039.691 | 11038.289 | 11095.281 | 11093.854 |
| 10.5 | 11085.866 | 11085.866 | 11102.022 | 11102.022 | 38.5 | 11037.454 | 11035.938 | 11094.497 | 11092.946 |
| 11.5 | 11084.688 | 11084.641 | | 11102.243 | 39.5 | 11035.181 | 11033.544 | 11093.669 | 11092.007 |
| 12.5 | 11083.453 | 11083.389 | | 11102.457 | 40.5 | 11032.874 | 11031.107 | 11092.812 | 11091.013 |
| 13.5 | 11082.160 | 11082.089 | | 11102.630 | 41.5 | 11030.528 | 11028.627 | 11091.917 | 11089.998 |
| 14.5 | 11080.832 | 11080.751 | | 11102.756 | 42.5 | 11028.149 | 11026.110 | 11090.967 | 11088.920 |
| 15.5 | 11079.470 | 11079.369 | | 11102.849 | 43.5 | 11025.734 | 11023.546 | 11089.998 | 11087.806 |
| 16.5 | 11078.068 | 11077.946 | | | 44.5 | 11023.287 | 11020.945 | 11089.007 | 11086.643 |
| 17.5 | 11076.626 | 11076.478 | | | 45.5 | 11020.802 | 11018.294 | 11087.965 | 11085.438 |
| 18.5 | 11075.143 | 11074.969 | | | 46.5 | 11018.294 | 11015.613 | 11086.893 | 11084.197 |
| 19.5 | 11073.618 | 11073.417 | 11102.960 | 11102.756 | 47.5 | 11015.736 | 11012.880 | 11085.784 | 11082.905 |
| 20.5 | 11072.050 | 11071.825 | 11102.849 | 11102.630 | 48.5 | 11013.142 | 11010.114 | 11084.641 | 11081.572 |
| 21.5 | 11070.458 | 11070.190 | 11102.723 | 11102.457 | 49.5 | 11010.522 | 11007.299 | 11083.453 | 11080.198 |
| 22.5 | 11068.817 | 11068.514 | 11102.543 | 11102.243 | 50.5 | 11007.870 | 11004.445 | 11082.242 | 11078.777 |
| 23.5 | 11067.143 | 11066.793 | 11102.328 | 11101.984 | 51.5 | 11005.182 | 11001.546 | 11080.994 | 11077.318 |
| 24.5 | 11065.428 | 11065.032 | 11102.078 | 11101.682 | 52.5 | 11002.462 | 10998.610 | 11079.713 | 11075.820 |
| 25.5 | 11063.672 | 11063.227 | 11101.787 | 11101.336 | 53.5 | 10999.709 | 10995.634 | 11078.397 | 11074.253 |
| 26.5 | 11061.880 | 11061.380 | 11101.454 | 11100.948 | 54.5 | 10996.925 | 10992.613 | 11077.042 | 11072.679 |
| 27.5 | 11060.051 | 11059.495 | 11101.078 | 11100.515 | 55.5 | 10994.107 | 10989.550 | 11075.659 | 11071.045 |
| 28.5 | 11058.181 | 11057.561 | 11100.674 | 11100.041 | 56.5 | 10991.249 | 10986.449 | 11074.253 | 11069.368 |

**TABLE 1**—*Continued*

$[11.1]^2\Pi_{3/2}(v'=0)–X^2\Pi_{3/2}(v''=0)$

| $J$ | $P_{ee}$ | $P_{ff}$ | $R_{ee}$ | $R_{ff}$ | $J$ | $P_{ee}$ | $P_{ff}$ | $R_{ee}$ | $R_{ff}$ |
|---|---|---|---|---|---|---|---|---|---|
| 57.5 | 10988.372 | 10983.304 | 11072.788 | 11067.652 | 75.5 | 10931.326 | 10919.607 | 11041.213 | |
| 58.5 | 10985.461 | 10980.116 | 11071.302 | 11065.893 | 76.5 | 10927.888 | 10915.674 | 11039.170 | |
| 59.5 | 10982.513 | 10976.889 | 11069.783 | 11064.086 | 77.5 | 10924.423 | 10911.694 | 11037.105 | |
| 60.5 | 10979.538 | 10973.622 | 11068.233 | 11062.242 | 78.5 | 10920.927 | 10907.658 | 11035.003 | |
| 61.5 | 10976.529 | 10970.311 | 11066.648 | 11060.344 | 79.5 | 10917.408 | 10903.588 | 11032.874 | |
| 62.5 | 10973.495 | 10966.955 | 11065.032 | 11058.417 | 80.5 | 10913.858 | | 11030.725 | |
| 63.5 | 10970.425 | 10963.567 | 11063.384 | 11056.408 | 81.5 | 10910.294 | | 11028.537 | |
| 64.5 | 10967.328 | 10960.137 | 11061.703 | 11054.422 | 82.5 | 10906.703 | | 11026.334 | |
| 65.5 | 10964.196 | 10956.658 | 11059.995 | 11052.352 | 83.5 | 10903.073 | | 11024.092 | |
| 66.5 | 10961.035 | 10953.141 | 11058.250 | 11050.256 | 84.5 | 10899.426 | | 11021.837 | |
| 67.5 | 10957.848 | 10949.583 | 11056.473 | 11048.106 | 85.5 | 10895.763 | | 11019.547 | |
| 68.5 | 10954.632 | 10945.983 | 11054.673 | 11045.910 | 86.5 | 10892.065 | | 11017.237 | |
| 69.5 | 10951.391 | 10942.343 | 11052.840 | 11043.676 | 87.5 | 10888.346 | | 11014.899 | |
| 70.5 | 10948.117 | 10938.659 | 11050.978 | 11041.402 | 88.5 | 10884.611 | | 11012.538 | |
| 71.5 | 10944.814 | 10934.935 | 11049.081 | 11039.069 | 89.5 | 10880.823 | | 11010.115 | |
| 72.5 | 10941.487 | 10931.174 | 11047.159 | 11036.699 | 90.5 | 10877.057 | | 11007.724 | |
| 73.5 | 10938.127 | 10927.355 | 11045.207 | 11034.284 | 91.5 | | | 11005.288 | |
| 74.5 | 10934.745 | 10923.508 | 11043.225 | | 92.5 | | | 11002.814 | |

$[11.1]^2\Pi_{3/2}\,(v'=0)–[0.25]^2\Sigma(v''=0)$

| $J$ | $Q_{fe}$ | $Q_{ef}$ | $P_{ee}$ | $P_{ff}$ | $R_{ee}$ | $R_{ff}$ |
|---|---|---|---|---|---|---|
| 2.5 | 10846.668 | | | | | |
| 3.5 | 10847.358 | | | | | |
| 4.5 | | | | | | |
| 5.5 | 10848.646 | | | | | |
| 6.5 | 10849.214 | | 10844.447 | | | |
| 7.5 | 10849.738 | 10835.845 | 10844.245 | | 10855.978 | |
| 8.5 | 10850.211 | 10834.610 | 10843.986 | | 10857.194 | |
| 9.5 | 10850.660 | 10833.265 | 10843.682 | | 10858.361 | |
| 10.5 | 10851.036 | 10831.928 | 10843.325 | 10824.216 | 10859.470 | |
| 11.5 | 10851.377 | 10830.541 | 10842.928 | 10822.088 | 10860.552 | |
| 12.5 | 10851.668 | 10829.099 | 10842.502 | 10819.927 | 10861.571 | |
| 13.5 | 10851.917 | 10827.616 | 10842.013 | 10817.702 | 10862.564 | |
| 14.5 | 10852.118 | 10826.090 | 10841.487 | 10815.440 | 10863.493 | |
| 15.5 | 10852.265 | 10824.526 | 10840.904 | 10813.140 | 10864.390 | 10837.465 |
| 16.5 | 10852.364 | 10822.906 | 10840.278 | 10810.795 | 10865.214 | 10836.615 |
| 17.5 | | 10821.250 | 10839.603 | 10808.394 | 10866.001 | 10835.733 |
| 18.5 | | 10819.544 | 10838.897 | 10805.960 | | 10834.799 |
| 19.5 | | 10817.795 | 10838.124 | 10803.476 | 10867.460 | 10833.825 |
| 20.5 | 10852.330 | 10816.005 | 10837.328 | 10800.952 | 10868.115 | 10832.807 |
| 21.5 | 10852.200 | 10814.157 | 10836.462 | 10798.385 | 10868.702 | 10831.748 |
| 22.5 | 10852.030 | 10812.290 | 10835.559 | 10795.758 | 10869.270 | 10830.636 |
| 23.5 | 10851.805 | 10810.362 | 10834.610 | 10793.105 | 10869.803 | 10829.480 |
| 24.5 | 10851.535 | 10808.394 | | 10790.400 | 10870.270 | 10828.287 |
| 25.5 | 10851.221 | 10806.384 | 10832.570 | 10787.652 | 10870.678 | 10827.044 |
| 26.5 | 10850.857 | 10804.326 | 10831.483 | 10784.866 | 10871.045 | 10825.767 |
| 27.5 | 10850.447 | 10802.228 | 10830.343 | 10782.021 | 10871.374 | 10824.408 |
| 28.5 | 10849.991 | 10800.088 | 10829.165 | 10779.163 | 10871.659 | 10823.059 |
| 29.5 | 10849.484 | 10797.904 | 10827.934 | 10776.229 | 10871.873 | 10821.643 |
| 30.5 | 10848.929 | 10795.673 | 10826.666 | 10773.273 | 10872.071 | 10820.177 |
| 31.5 | 10848.330 | 10793.405 | 10825.348 | 10770.265 | | 10818.659 |
| 32.5 | 10847.682 | 10791.091 | 10823.985 | 10767.213 | | 10817.111 |
| 33.5 | 10846.993 | 10788.736 | 10822.564 | 10764.127 | | 10815.517 |
| 34.5 | 10846.254 | 10786.335 | 10821.106 | 10760.992 | | 10813.906 |
| 35.5 | 10845.464 | 10783.893 | 10819.600 | 10757.812 | | 10812.204 |
| 36.5 | 10844.634 | 10781.404 | 10818.045 | 10754.589 | | 10810.476 |

**TABLE 1**—*Continued*

| $[11.1]^2{}_{3/2}(v'=0)$–$[0.25]^2\Sigma(v''=0)$ | | | | | | |
|---|---|---|---|---|---|---|
| $J$ | $Q_{fe}$ | $Q_{ef}$ | $P_{ee}$ | $P_{ff}$ | $R_{ee}$ | $R_{ff}$ |
| 37.5 | 10843.747 | 10778.885 | 10816.442 | 10751.327 | | 10808.689 |
| 38.5 | 10842.815 | 10776.316 | 10814.801 | 10748.026 | | 10806.894 |
| 39.5 | 10841.839 | 10773.705 | 10813.111 | 10744.672 | | 10805.049 |
| 40.5 | 10840.812 | 10771.052 | 10811.374 | 10741.288 | | 10803.124 |
| 41.5 | 10839.735 | 10768.359 | 10809.586 | 10737.859 | | 10801.208 |
| 42.5 | 10838.618 | 10765.627 | 10807.758 | 10734.386 | | 10799.218 |
| 43.5 | 10837.465 | 10762.845 | 10805.878 | 10730.870 | | 10797.185 |
| 44.5 | 10836.232 | 10760.029 | 10803.953 | 10727.316 | | 10795.120 |
| 45.5 | 10834.960 | 10757.170 | 10801.986 | 10723.722 | | 10793.015 |
| 46.5 | 10833.633 | 10754.270 | 10799.968 | 10720.074 | | 10790.854 |
| 47.5 | 10832.294 | 10751.328 | 10797.904 | 10716.397 | | |
| 48.5 | 10830.889 | 10748.346 | 10795.799 | 10712.683 | | |
| 49.5 | 10829.435 | 10745.325 | 10793.645 | 10708.916 | | |
| 50.5 | 10827.933 | 10742.262 | 10791.440 | 10705.114 | | |
| 51.5 | 10826.378 | 10739.157 | 10789.189 | 10701.268 | | |
| 52.5 | 10824.780 | 10736.016 | 10786.900 | 10697.386 | | |
| 53.5 | 10823.136 | 10732.832 | 10784.560 | 10693.461 | | |
| 54.5 | 10821.435 | 10729.612 | 10782.175 | 10689.503 | | |
| 55.5 | 10819.707 | 10726.347 | 10779.747 | 10685.494 | | |
| 56.5 | 10817.901 | 10723.046 | 10777.267 | 10681.450 | | |
| 57.5 | 10816.067 | 10719.706 | 10774.740 | 10677.366 | | |
| 58.5 | 10814.158 | 10716.325 | 10772.174 | 10673.240 | | |
| 59.5 | | 10712.907 | 10769.562 | 10669.074 | | |
| 60.5 | | 10709.448 | 10766.901 | 10664.872 | | |
| 61.5 | | | 10764.193 | 10660.629 | | |
| 62.5 | | | 10761.440 | | | |
| 63.5 | | | 10758.645 | | | |
| 64.5 | | | 10755.804 | | | |
| 65.5 | | | 10752.915 | | | |
| 66.5 | | | 10749.978 | | | |
| 67.5 | | | 10746.991 | | | |
| 68.5 | | | 10743.976 | | | |
| 69.5 | | | 10740.909 | | | |

### (c) The 10 850 cm$^{-1}$ Transition

The nature of the $[11.1]^2\Pi_{3/2}$ state is confirmed by the fact that we observed two band heads located at 10 852 and 10 252 cm$^{-1}$. It is obvious that the first one is the $Q_{fe}$ head of the $[11.1]^2\Pi_{3/2}$–$[0.25]^2\Sigma$ transition and that the second one is the $R$ head of the $[11.1]^2\Pi_{3/2}$–$[0.83]^2\Delta_{5/2}$ transition. This second transition is weak and overlapped by an intense transition. The transition

**TABLE 2**
**Molecular Constants (in cm$^{-1}$) of the $v = 0$ and $v = 1$ Levels of the Electronic States of NiF (All Uncertainties Are 1$\sigma$)**

| | $T_0$ | $B_0$ | $D_0 \times 10^7$ | $a$ | $p$ | $p_J \times 10^5$ | $\gamma$ | $\gamma_D \times 10^5$ |
|---|---|---|---|---|---|---|---|---|
| $[12.0]^2\Phi_{7/2}$ | 12008.9241(10) | 0.365925(23) | 5.137(61) | | | | | |
| | 12629.8392(32)[c] | 0.363190(70)[c] | 4.966(88)[c] | | | | | |
| $[11.1]^2\Pi_{3/2}$ | 11096.0471(15) | 0.3671132(25) | 5.063(35) | 0.0193(45) | −0.00175(30) | 0.3151(40) | | |
| $[0.83]A^2\Delta_{5/2}$ | 829.4761[b] | 0.388546(24) | 5.410(64) | | | | | |
| | 1482.7901(25)[c] | 0.385166(45)[c] | 5.230(95)[c] | | | | | |
| $[0.25]^2\Sigma$ | 251.2616(11) | 0.39001840(85) | 5.616(14) | | | | −0.960075(34) | 1.8432(20) |
| | | *0.390016166(37)*[a] | *5.58023(93)*[a] | | | | *−0.9597221(18)*[a] | *1.79087(32)*[a] |
| $X^2\Pi_{3/2}$ | 0 | 0.38781570(73) | 6.141(12) | | | −2.3533(25) | | |
| | | *0.387816528(28)*[a] | *6.15136(67)*[a] | | | *−2.31740(33)*[a] | | |

[a] From Ref. (*1*).
[b] From Ref. (*5*).
[c] Parameters of the $v = 1$ levels.

at 10 852 $cm^{-1}$, however, can be easily analyzed thanks to the known term values of the two states involved. In a first step we calculated the expected positions of the lines on the basis of the term values of the $[11.1]^2\Pi_{3/2}$ state and of the $[0.25]^2\Sigma$ state (*1, 5*). About 280 lines belonging to the six expected branches have been identified, despite the weakness of the experimental spectrum (Table 1). We added these data to those of the stronger $[11.1]^2\Pi_{3/2}$–$X^2\Pi_{3/2}$ transition, and we included the microwave data of the $[0.25]^2\Sigma$ state (*1*). The constants listed in Table 2 for the $[11.1]^2\Pi_{3/2}$ state are derived from the final fit, which includes 617 experimental lines.

## IV. CONCLUSION

In this paper we report the first analysis of near-infrared electronic transitions of NiF. Two new electronic states have been identified. As predicted by ligand field calculations, a $[12.0]^2\Phi_{7/2}$ state has been identified. This supports the theoretical energy level diagram published by Carette *et al.* (*6*). We note that the group of states correlating with the $[3d^8(3\mathrm{F})4s]^2F$ atomic state of $Ni^+$ has to be increased by about 5000 $cm^{-1}$ to agree with the experimental position of the $[12.0]^2\Phi_{7/2}$ state. Such a discrepancy between experimental and calculated positions of the states may appear to be considerable. We must note that calculations based on ligand field theory (*6*) enabled the construction of a rough energy level diagram. The aim was to show that the molecular electronic states are strongly correlated with the atomic structure of the $Ni^+$ ion. When some experimental positions of states are known then the ligand field predictions can be improved, as observed for the upper states of the visible transitions of NiF (*5*). In Ref. (*5*), the lack of information on the near-infrared transitions resulted in reduced accuracy for the predictions for the lower-lying excited states. Nevertheless we can conclude that the electronic states responsible for the infrared transitions of NiF are correlated to the $[3d^8(3\mathrm{F})4s]^2F$ atomic parent state of $Ni^+$ as confirmed by the presence of a $^2\Phi$ electronic state, and we can expect that the six close-lying spin–orbit components correlating with the $^2F$ atomic state of $Ni^+$ are responsible for the numerous bands observed in the near infrared region of the NiF spectrum.

## ACKNOWLEDGMENTS

We thank the Natural Sciences and Engineering Research Council of Canada for financial support. The Centre d'Etudes et de Recherches Lasers et Applications is supported by the Ministère Chargé de la Recherche, the Région Nord-Pas de Calais, and the Fond Européen de Développement Economique des Régions.

## REFERENCES


1. M. Tanimoto, T. Sakamaki, and T. Okabayashi, *J. Mol. Spectrosc.* **207,** 66–69 (2001).
2. Y. Chen, J. Jin, C. Hu, X. Yang, X. Ma, and C. Chen, *J. Mol. Spectrosc.* **203,** 37–40 (2000).
3. J. Jin, Y. Chen, C. Hu, X. Yang, Q. Ran, and C. Chen, *J. Mol. Spectrosc.* **208,** 18–24 (2001).
4. J. Jin, Q. Ran, X. Yang, Y. Chen, and C. Chen, *J. Phys. Chem. A* **105,** 11177–11182 (2001).
5. Y. Krouti, T. Hirao, C. Dufour, A. Boulezhar, B. Pinchemel, and P. F. Bernath, *J. Mol. Spectrosc.* (*submitted*).
6. P. Carette, C. Dufour, and B. Pinchemel, *J. Mol. Spectrosc.* **161,** 323–335 (1993).
7. T. Hirao, B. Pinchemel, and P. F. Bernath, *J. Mol. Spectrosc.* **202,** 213–222 (2000).
8. G. Norlén, *Phys. Scr.* **8,** 249–268 (1973).
9. I. Kovács, "Rotational Structure in the Spectra of Diatomic Molecules." Adam Hilger, London, 1969.
10. C. Focsa, C. Dufour, and B. Pinchemel, *J. Mol. Spectrosc.* **182,** 65–71 (1997).